

# RSC Advances



This is an *Accepted Manuscript*, which has been through the Royal Society of Chemistry peer review process and has been accepted for publication.

*Accepted Manuscripts* are published online shortly after acceptance, before technical editing, formatting and proof reading. Using this free service, authors can make their results available to the community, in citable form, before we publish the edited article. This *Accepted Manuscript* will be replaced by the edited, formatted and paginated article as soon as this is available.

You can find more information about *Accepted Manuscripts* in the [Information for Authors](#).

Please note that technical editing may introduce minor changes to the text and/or graphics, which may alter content. The journal's standard [Terms & Conditions](#) and the [Ethical guidelines](#) still apply. In no event shall the Royal Society of Chemistry be held responsible for any errors or omissions in this *Accepted Manuscript* or any consequences arising from the use of any information it contains.

## ARTICLE

## Degradable, Silyl Ether Thiol-Ene Networks

Taylor Ware <sup>††1</sup>, Abby R. Jennings <sup>‡2</sup>, Zahra S. Bassampour<sup>2</sup>, Dustin Simon<sup>1</sup>, David Y. Son <sup>\*2</sup> and Walter Voit <sup>\*1</sup>

Cite this: DOI: 10.1039/x0xx00000x

Received 00th January 2012,  
Accepted 00th January 2012

DOI: 10.1039/x0xx00000x

www.rsc.org/

A system of multifunctional silyl ether containing alkene and thiol monomers are synthesized and polymerized into uniform degradable networks with widely tunable thermomechanical properties. The glass transition temperature of the hydrolytically unstable networks can be controlled between -60 °C and 40 °C. Near total degradation is observed and the rate of degradation is controlled to occur between hours and months. Dynamic mechanical analysis, mass loss, uniaxial compression testing, multinuclear NMR spectroscopy, and gas chromatography–mass spectrometry are utilized to characterize the degradation of these networks. Importantly, this system of materials allows for rapid hydrolytic degradation that is not preceded by swelling. These degradable polymers are demonstrated to be compatible with microfabrication techniques, namely photolithography. As a demonstration, biodegradable device cortical electrodes were fabricated and electrochemically characterized on silyl ether substrates.

### Introduction

Hydrolytically degradable polymers have been designed and developed towards a wide variety of biomedical applications including scaffolds for tissue engineering, orthopedic implants and drug delivery systems.<sup>1</sup> A number of degradable moieties have been explored and the resulting polymeric materials tuned to achieve a wide range of mechanical properties and degradation profiles. Aliphatic polyesters, such as poly(lactic acid) and poly(caprolactone), have received significant attention as tunable polymers that degrade on the order of years under physiological conditions.<sup>2</sup> Although hydrophilic aliphatic polyesters may undergo degradation more rapidly, poly(anhydrides) and poly(ortho esters) provide significantly more labile functionalities which can yield materials that degrade on the order of minutes to days. More recently, other highly labile moieties such as silyl ethers and silyl esters have been incorporated into polymeric materials to induce hydrolytic degradation.<sup>3–6</sup> Silyl ethers are commonly utilized to protect alcohols and are readily hydrolyzed, yielding a silanol and an alcohol. Importantly, neither of these byproducts is considered inherently toxic or leads to drastic changes in the pH of the surrounding medium.<sup>5</sup> Recently, the synthesis of multifunctional thiols containing silyl ether linkages was achieved through the selective condensation of the alcohol group of mercaptoalcohols with chlorosilanes.<sup>7</sup> The ready availability of these thiols and the existence of highly efficient “thiol-click” reactions (reactions of thiols with alkenes, epoxides, and isocyanates, among others) provide a facile and novel entry to a wide variety of previously unknown degradable

poly(silyl ethers), which provides a rich toolset with which to separate fundamental phenomena that govern network degradation in aqueous environments.

The group of click reactions originally described by Sharpless et al. did not include the thiol-click reactions, but these thiol-click reactions are now widely considered to possess similar characteristics: namely, the reactions can be carried out to high yield under mild reaction conditions.<sup>8,9</sup> In particular, the step growth, free radical polymerization of multifunctional thiols with multifunctional alkenes (thiol-ene) has received significant attention. The resulting polymer networks are considerably more homogeneous and possess lower cure stresses compared to acrylic networks.<sup>10,11</sup> These advantages have been recognized in the stimuli-responsive polymer literature, and have led to a number of thiol-ene based smart polymeric materials that exhibit shape memory, tunable degradation, and photoplasticity.<sup>12–14</sup> In addition, certain thiol-ene substrates are known to be compatible with microelectronics processing, enabling stimuli-responsive flexible electronics.<sup>15</sup> Specifically, intracortical electrode arrays can be fabricated utilizing photolithography on thermoset substrates that are glassy for penetration of the outer layers of cortical tissue, and subsequently undergo a significant reduction in modulus. Compliant intracortical implants have been demonstrated to exhibit a reduction in the immune response and may offer a strategy to improve device performance.<sup>16,17</sup> It has also been shown that device size plays an important role in minimizing the immune response to these indwelling electrodes.<sup>18</sup> The use of insertion shuttles to deliver small electrode arrays has been previously discussed, but the fabrication of thin-film electronics directly on biodegradable substrates has not been demonstrated.<sup>19,20</sup>

In this work, a series of silyl ether multifunctional alkene and thiol monomers were synthesized and polymerized in bulk using thiol-ene chemistry. The resulting polymer networks were thermomechanically characterized, and the degradation of these materials was monitored in simulated physiological conditions through mass change, quasi-static mechanical testing,  $^1\text{H}$  NMR spectroscopy, and gas chromatography (GC-MS). Through these methods, the effect of network structure on thermomechanical properties and degradation is highlighted.

## Results

The goal of this work was to design and characterize a system of amorphous poly(silyl ether) thermosets that tunably degrade in physiological conditions through hydrolysis. To this end, six silyl ether containing multifunctional thiols or alkenes were designed and synthesized. The monomers were designed such that by controlling steric hindrance around the silyl ether core of each monomer, the extent and rate of both initial crosslinking and final degradation could be precisely controlled once these monomers were incorporated into a polymer network. This series of monomers was combined with two commercially available monomers to yield a series of polymers through free-radical thiol-ene chemistry. **Figure 1a** is a pictorial representation of the commercially available monomers used in this study (**3,8**) and the custom synthesized monomers (**1,2,4-7**). Monomers **1** and **2** were synthesized using known methods.<sup>21,22</sup> **Figure 1b** illustrates the synthetic strategy used for the synthesis of monomers **4-7**.<sup>7</sup> For these monomers, the appropriate chlorosilane was added to a cold solution of 2-mercaptoethanol and triethylamine. The resulting suspension was stirred under nitrogen at room temperature overnight, and the crude products were isolated by first removing the amine salt by vacuum filtration and then removing all volatiles through rotary evaporation. Monomers **4** and **5** were purified by distillation under reduced pressure.

Initially, four compositions were synthesized in which both the thiol and alkene monomers possessed the reactive groups connected to the central atom through a hydrolysable silyl ether linkage. Namely, both tetra-allyl (**1**) and tri-allyl (**2**) monomers were polymerized with a tetra-thiol (**4**) and a tri-thiol (**5**). DMA, shown in **Figure 2a,b**, demonstrated each of these networks to be elastomeric at room temperature with a distinct and narrow glass transition temperature ( $T_g$ ) ranging from  $-55$  °C to  $-28$  °C.  $T_g$ , denoted as the peak of  $\tan \delta$ , and crosslink density, proportional to the rubbery plateau modulus above the  $T_g$ , both scale with the average functionality of the monomer. Each of the silyl ether containing networks characterized thermomechanically in **Figure 2a,b** underwent significant degradation upon exposure to physiological conditions. Degradation was monitored over 6 weeks by measuring both the equilibrium mass (**Figure 2c**) and mass of polymer after drying (**Figure 2d**) of samples that had been exposed to simulated physiological conditions. It should be noted that each of these samples never significantly increased in mass, and the

equilibrium mass change was always negative. Degradation of the two networks containing **4** proceeded rapidly. The **4+2** sample reached a maximum mass loss of  $\sim 80\%$  in 12 hours, and the **4+1** sample reached a similar plateau between 1 day and 1 week. Samples polymerized with the methyl-substituted thiol, **5**, degraded more slowly. It should be noted that total dissolution of the polymer was not observed for any of these samples. Instead, the sample degraded to a loosely coherent, low density cloudy gel.

To better understand the degradation processes, quasi-static compression in phosphate buffered saline (PBS) at  $37$  °C was performed on both networks containing **4**. Representative data of the stress-strain behavior for both the **4+1** (**Figure 3a**) and the **4+2** (**Figure 3b**) samples indicate a reduction in modulus (slope of the stress-strain curve) upon exposure to physiological conditions. After 6 hours for **4+2** and after 48 hours for **4+1**, the samples no longer supported the small preload of  $0.03$  MPa without significant deformation or failure.

In addition to this mechanical probe of network properties, the degradation products were identified. Initially, the degradation products of **4+2** were monitored by GC-MS (**Figure 3c**). The top chromatogram shows the final analysis of the degraded network. The chromatogram contains a significant peak at approximately 8.0 minutes, corresponding to the major degradation product, and a very small shoulder that appears around 7.8 minutes. The model degradation compound shown underneath exhibits a similar profile with a major peak near 8.1 minutes and a minor peak around 7.5 minutes. The bottom two chromatograms correspond to 2-mercaptoethanol and allyl alcohol, and contain one major peak each at 2.9 and 1.5 minutes respectively. After the GC-MS analysis of **4+2** was complete, the degradation products were further evaluated using  $^1\text{H}$  NMR spectroscopy by extracting the aqueous layer with  $\text{CDCl}_3$  (**Figure 3d**). The top spectrum corresponds to the degraded network. Significant signals not due to the degradation products are appropriately labeled. The spectra of the model degradation compound and the respective starting materials are shown below the degraded network.

The networks characterized in **Figures 2** and **3** are all elastomeric and highly crosslinked. In order to synthesize networks which are glassy at room temperature, a rigid, hydrolytically stable tri-allyl monomer (**3**) was polymerized with a series of silyl ether thiols. Multi-functional thiol **4** and thiols with non-hydrolysable substituents on the silicon atom (methyl (**5**), phenyl (**6**), diphenyl (**7**)) were synthesized and polymerized in bulk with **3**. Each of these monomers is miscible with **3** at room temperature. As shown by DMA in **Figure 4a,b**, the  $T_g$ 's of these networks range between  $28$  °C and  $40$  °C, with **4+3** having the highest  $T_g$  and crosslink density. The rubbery modulus (proportional to crosslink density) trends negatively with the molecular weight per thiol group. The rubbery modulus was greater than one order of magnitude larger for the **4+3** composition as compared to the **7+3** composition due to the effect a tetra-functional thiol has on crosslink density relative to a di-functional thiol. Equilibrium mass and mass loss were monitored for each network as a

function of time during exposure to physiological conditions (**Figure 4c,d**). Each network exhibited significant degradation and the equilibrium mass at each measured time point was less than the initial mass. Over 6 weeks, **3+6** lost  $29\% \pm 1\%$ , while each of the other samples degraded between approximately 60 and 80%. However, it is important to remember that each crosslink in the network contains a single silyl ether linkage, begetting networks that can ultimately undergo near complete degradation.

In order to study the mass loss in networks that do not contain readily hydrolysable silyl ether linkages at every branch point in the network, compositions were synthesized that contained a tri-functional mercaptopropionate, **8**. The alkene, **3**, was copolymerized with a mixture of **8** and a degradable thiol, either **4** or **5**. Silyl ether content was controlled so that on average 0/3, 1/3, 2/3 or 3/3 of the resulting network branches were readily hydrolysable. DMA of the resulting homogenous polymer networks is shown in **Figure 5**. In networks containing either **4** or **5**,  $T_g$  decreased and rubbery modulus increased with increasing silyl ether content. In addition, the  $T_g$  and rubbery modulus for **3+8+4** networks were higher than the measured values for **3+8+5** networks for a given silyl ether content. As seen in **Figure 6a,b**, mass loss increased with increasing silyl ether content. The control composition **3+8** exhibited a slight swelling with no associated mass loss over the observed period of 6 weeks, as has been reported elsewhere.<sup>15</sup> In compositions with one-third silyl ether content, only slight swelling was observed. Mass loss of approximately 25% was observed for compositions with two-thirds silyl ether thiols. Significant differences in degradation behavior were not observed in the networks containing the tetra-functional thiol (**4**) or the tri-functional thiol (**5**). In addition to mechanical and gravimetric analysis of silyl ether thiol-ene materials, the degradation products were also monitored.

A degradation analysis of **5+3** was performed by first monitoring the degradation by GC-MS (**Figure 6c**). The top chromatogram represents the final analysis of the degraded network, and contains two peaks at approximately 10.2 and 14.7 minutes. The chromatogram of a model degradation compound is shown below the degraded network and exhibits a similar profile. It should be noted that the expected major degradation product cannot be analyzed by GC-MS due to its lack of volatility. The bottom two chromatograms correspond to 2-mercaptoethanol and **3**, and contain one major peak each at 2.9 and 10.2 minutes, respectively. After the GC-MS analysis of **5+3** was complete, the aqueous layer was extracted with  $\text{CDCl}_3$  and the degradation products further analyzed by  $^1\text{H}$  NMR spectroscopy (**Figure 6d**). The top spectrum shows the final analysis of the degraded network. Significant signals not due to the degradation products are appropriately labeled. The spectrum of the major model degradation compound, which was obtained by the thiol-ene reaction of **3** and three equivalents of 2-mercaptoethanol, is shown below the degraded polymer. The bottom two spectra correspond to 2-mercaptoethanol and **3**, respectively. Understanding the

degradation of the silyl ether we sought to fabricate partially-degradable bioelectronics.

The suitability of **4+3** to serve as a degradable substrate for implantable electronics, such as arrays of microelectrodes, was evaluated. This composition was chosen due to its combination of a relatively high  $T_g$  and near complete degradation. The idealized cross section of the fabricated microelectrode arrays is schematized in **Figure 7a**. Utilizing Parylene-C as the dielectric and gold as both the conductor and electrode material, devices were fabricated with standard photolithography. As an example of the devices that can be fabricated, optical micrographs in **Figure 7b,c** depict two arrays of microelectrodes nominally designed to record neural activity from the auditory cortex of a rat. **Figure 7b** is an example of an electrode array designed to perform electrocorticography, while **Figure 7c** is similar to penetrating intracortical multielectrode arrays. Electrochemical impedance spectroscopy of a representative  $2000 \mu\text{m}^2$  gold electrode is shown in **Figure 7d**. After immersion in simulated physiological conditions the substrate degrades leaving only Parylene-C encapsulated microelectrodes. As a result, the device undergoes a reduction in thickness from  $35 \mu\text{m}$  to just over  $1 \mu\text{m}$ .

## Discussion

Polymers in biomedical devices that undergo degradation in physiological conditions interact with the surrounding tissue through leaching of degradation products and changes in modulus and geometry in a time-dependent manner. In this work, a strategy is presented to allow for precise control over this temporal response in a system of materials that may be useful in applications that require precise degradation profiles, control of glass transition temperature, and compatibility with photolithography, such as the fabrication of minimally-invasive implantable arrays of microelectrodes. Wide control over the glass transition temperature, crosslink density and degradation of silyl ether containing polymer networks formed through the radical thiol-ene reaction is demonstrated. The potential utility of these materials to serve as substrates for electronics that can withstand photolithography for the processing of microelectronics, deliver these electronics into soft tissue, and subsequently degrade leaving behind a minimally invasive implant is also discussed.

Silyl ether thiols, monomers **4-7**, were obtained through the selective reactions of chlorosilanes and 2-mercaptoethanol. In these reactions, the chlorosilane reacts exclusively with the hydroxyl functionality of the 2-mercaptoethanol molecule, allowing one to easily obtain thiol terminated monomers. Furthermore, there are a wide variety of commercially available and synthesizable chlorosilanes that can be employed as starting materials for this reaction. Reaction conditions are mild and product purification, when necessary, can usually be performed by vacuum distillations. This provides a straightforward methodology to alter the functional groups attached to the central silicon atom and in turn, tune the properties of the resulting material.

Model poly(silyl ether)s were synthesized in bulk from the synthesized silyl ether thiols and silyl ether alkenes. Due to the hydrolysable nature of the Si-O bond present within the networks formed from 4+2 or 4+1, each composition undergoes a rapid reverse gelation process as indicated by the reduction in modulus (**Figure 3a,b**) and mass loss (**Figure 2d**) of these elastomers, in which the degradation products are readily predictable. As shown in **Figure 3e**, the major degradation product expected from 4+2 is 3-(2-hydroxyethylsulfanyl)propan-1-ol, or compound **9**. To verify the presence of this compound in the degraded network, **9** was synthesized via the thiol-ene reaction of allyl alcohol with 2-mercaptoethanol. As shown in **Figure 3c**, the model degradation compound exhibited two peaks in the chromatogram. The more prominent peak observed in the chromatogram yielded a mass spectrum that corresponded to **9** (see **Figure S 7**, Supporting Information). When performing thiol-ene reactions, there is a small percentage of thiol that adds across the interior carbon atom of the alkene, yielding what is known as the alpha product. The minor peak observed in the chromatogram of the model compound had a mass spectrum that corresponded to the alpha product (see **Figure S 8**, Supporting Information). Since the chromatogram of the degraded sample shown in **Figure 3c** exhibited the same characteristic peaks as the model compound, it can be inferred that the degraded material contained mostly **9** and a very small amount of the alpha product.

GC-MS analysis is only appropriate for the detection of lower molecular weight compounds. Hence, an extraction was performed on the degraded sample that was used in the GC-MS study and a  $^1\text{H}$  NMR spectral analysis was performed on the aqueous layer. When comparing the spectra of the degraded sample and the model compound, similar peaks are present. The only discrepancy observed in the spectra is the location and appearance of the hydroxyl chemical shifts; however, it is well known that the general appearance and placement of hydroxyl protons can fluctuate and is dependent on the chemical environment. The presence of the alpha product was also verified in the  $^1\text{H}$  NMR spectral experiment by the appearance of a characteristic upfield doublet, which corresponds to the protons of the methyl group. These observations further support the notion that the major degradation product is **9**, containing a small amount of the alpha product. The acetone and dichloromethane seen in the spectrum were externally introduced into the sample during the GC-MS study. The degraded sample was monitored daily over a three week period, which allowed for enough solvent to be introduced such that it could be detected in the  $^1\text{H}$  NMR spectral analysis. The lack of 2-mercaptoethanol or allyl alcohol in the degradation sample indicates that monomer conversion was nearly complete.

Although the rapid degradation and elastomeric nature of the previously described materials may prove useful for certain applications, previous work has demonstrated that these low modulus materials yield devices without the requisite stiffness necessary to penetrate soft tissue and deliver microelectronics. To synthesize materials that fit in this property space but that

can also degrade at controlled time points following implantation, the high flexibility of the silyl ether and thio-ether must be overcome to move the  $T_g$  above ambient temperatures. Several changes were made to the model networks characterized in **Figure 2-3**. Degradable silyl ether alkenes were replaced with **3** to increase the rigidity of the network, shifting the  $T_g$  upward by nearly 100 °C. As with the 4+2 network, the major degradation products of the network formed from 5+3 were predicted and verified. As shown in **Figure 6e**, the major product expected is 1,3,5-tris[3-(2-hydroxyethylsulfanyl)propyl]-1,3,5-triazinane-2,4,6-trione, or compound **10**.

To verify the presence of this compound in the degraded network, **10** was synthesized via the thiol-ene reaction of **3** with three equivalents of 2-mercaptoethanol. Due to its higher molecular weight and boiling point, compound **10** could not be analyzed via GC-MS. Additionally, a second model degradation product was prepared by reacting **3** with one equivalent of 2-mercaptoethanol. This thiol-ene reaction would produce a mixture of compounds including unreacted **3**, **10**, and compounds **11** and **12** shown in **Figure 6e**. Of these products, only **3** and **11** are detectable by GC-MS.

As shown in **Figure 6c**, the degradation sample from 5+3 exhibited two peaks in the chromatogram. The smaller peak appeared at the same retention time as that of pure **3** and yielded a mass spectrum that corresponded to **3** (see **Figure S 9**, Supporting Information). The retention time of the larger peak and its mass spectrum corresponded to **11** (see **Figure S 10**, Supporting Information). Thus, it can be deduced that the degraded material contains some **11**, a small amount of unreacted **3**, and most likely some **12**, although **12** cannot be observed using GC-MS. The trace amounts of **3** and partially reacted **11** in the GC chromatogram may be attributed to a slight stoichiometric excess of alkene due to difference in monomer purity. The presence of **11** and unreacted **3** in the degraded sample implies that network formation in this case is incomplete (but mostly complete; see  $^1\text{H}$  NMR spectral analysis below). It is believed that as the network is forming, **3** and partially reacted **3** becomes trapped by the vitrification of the polymer network and as the sample degrades, are released. It is critical to understand what degradation products emerge and how well they are tolerated *in vivo* to ensure that they do not cause unwanted effects. The scope of that effort warrants further inquiry beyond the basic identification of products from these systems as confirmed by GC-MS and  $^1\text{H}$  NMR spectroscopy.

Since the identification of all degradation products could not be confirmed in the GC-MS analysis, an extraction was performed on the degraded sample and a  $^1\text{H}$  NMR spectral analysis performed on the aqueous layer. When comparing the spectra of the degraded sample and model compound **10**, similar peaks are present (**Figure 6d**). As with the  $^1\text{H}$  NMR spectral study of the degraded sample obtained from 4+2, the major difference between the degraded sample and the model compound is the location and appearance of the hydroxyl protons. The presence of unreacted alkene groups attributed to **11**, **12**, and unreacted **3**

was also verified in the  $^1\text{H}$  NMR spectral experiment, although based on the integration of the alkene signals, the amount of unreacted alkene is small. These observations support the prediction of **10** being the major degradation product.

The present work presents the first published example of silyl ether based thiol-click networks. It is hoped that these widely tunable degradable thermosets may find use in both biomedical and industrial applications. Recently, there has been interest in fabricating transient electronics on degradable polymer substrates.<sup>23</sup> The polymers discussed in this work distinguish themselves from existing biodegradable materials by compatibility with microfabrication techniques, if the substrate is protected from extended exposure to water. Gold electrodes directly fabricated on these degradable substrates have similar electrochemical performance to other previously reported gold microelectrodes.<sup>15</sup> After fabrication, the substrate supporting the flexible electronic device degrades without first swelling significantly, so as not to damage the encapsulated thin film electronics. Previously published work has demonstrated the suitability of amorphous thiol-ene networks to serve as substrates for the fabrication of flexible electronics capable of changing modulus, from glassy to elastomeric, in response to physiological conditions. This work extends the physiological response of the substrate to include near total degradation.

## Experimental

### Materials

1,3,5-triallyl-1,3,5-triazine-2,4,6-(1H,3H,5H)-trione (TATATO) and 2,2-dimethoxy-2-phenylacetophenone (DMPA) were purchased from Sigma Aldrich. Tris[2-(3-mercaptopropionyloxy)ethyl] isocyanurate (TMICN) was purchased from Wako Chemicals. Phosphate buffered saline (PBS) with a pH of 7.4 was purchased from Fisher Scientific. These chemicals were used as received without further purification. All device fabrication processing steps, except polymer synthesis, were performed in a Class 10,000 cleanroom. The trichlorophenylsilane and dichlorodiphenylsilane were purchased from Acros Organics. The tetrachlorosilane, trichloromethylsilane, and allyl alcohol were purchased from Alfa Aesar. All chlorosilanes and the allyl alcohol were distilled over magnesium turnings prior to use. The triethylamine was purchased from TCI and distilled over calcium hydride prior to use. The ether was purchased from EMD and dried over activated 4 Å molecular sieves. The 2-mercaptoethanol was purchased from Amersco and used as received.

### Monomer synthesis and characterization

The  $^1\text{H}$ ,  $^{13}\text{C}$ , and  $^{29}\text{Si}$  NMRs were measured on a JOEL 500 MHz NMR spectrometer and chemical shifts are reported in parts per million referenced to tetramethylsilane. Elemental analyses were obtained using a CE Elantech Thermo-Finnigan Flash 1112 elemental analyzer.

Monomers **1** and **2** were synthesized using known methods.<sup>21,22</sup> The syntheses and characterization data for monomers **4** and **5** have been reported previously.<sup>7</sup>

### 2-[PHENYL-BIS(2-SULFANYLETHOXY)SILYL]OXYETHANETHIOL

Monomer **6** was synthesized employing the same method as monomers **4** and **5**, using ether (400 mL), triethylamine (18.20 mL, 0.13 mol), 2-mercaptoethanol (9.20 mL, 0.13 mol), and trichlorophenylsilane (7.00 mL, 0.044 mol). The product was obtained as a clear and colorless liquid (12.67 g, 86.0%).  $^1\text{H}$ -NMR (500 MHz,  $\text{CDCl}_3$ )  $\delta$  7.68–7.66 (m, aromatic, 2H), 7.49–7.38 (m, aromatic, 3H), 3.95 (t,  $-\text{OCH}_2\text{CH}_2\text{SH}$ , 6H,  $^3J = 6.3$  Hz), 2.71 (d,t,  $-\text{OCH}_2\text{CH}_2\text{SH}$ , 6H,  $^3J = 7$ , 6.3 Hz), 1.54 (t,  $-\text{OCH}_2\text{CH}_2\text{SH}$ , 3H,  $^3J = 8.3$  Hz).  $^{13}\text{C}$ -NMR (125 MHz,  $\text{CDCl}_3$ )  $\delta$  134.9 (aromatic C), 131.1 (aromatic C), 129.5 (aromatic C), 128.3 (aromatic C), 65.2 ( $-\text{OCH}_2\text{CH}_2\text{S}-$ ), 27.0 ( $-\text{OCH}_2\text{CH}_2\text{S}-$ )  $^{29}\text{Si}$ -NMR (99 MHz,  $\text{CDCl}_3$ ):  $\delta$  -57.7 (PhSi-). EA calcd for  $\text{C}_{12}\text{H}_{20}\text{O}_3\text{S}_3\text{Si}$  C 42.82, H 5.99; found C 42.60, H 6.07.

### 2-[DIPHENYL(2-SULFANYLETHOXY)SILYL]OXYETHANETHIOL

Monomer **7** was synthesized by employing the same method as **6**, using ether (200 mL), triethylamine (9.30 mL, 0.067 mol), 2-mercaptoethanol (4.70 mL, 0.067 mol), and dichlorodiphenylsilane (7.00 mL, 0.033 mol). The product was obtained as a clear and colorless liquid (10.02 g, 89.5%).  $^1\text{H}$ -NMR (500 MHz,  $\text{CDCl}_3$ )  $\delta$  7.68–7.66 (m, aromatic, 4H), 7.47–7.38 (m, aromatic, 6H), 3.92 (t,  $-\text{OCH}_2\text{CH}_2\text{SH}$ , 4H,  $^3J = 7$  Hz), 2.72 (d,t,  $-\text{OCH}_2\text{CH}_2\text{SH}$ , 4H,  $^3J = 8$ , 6 Hz), 1.57 (t,  $-\text{OCH}_2\text{CH}_2\text{SH}$ , 2H,  $^3J = 8$  Hz).  $^{13}\text{C}$ -NMR (125 MHz,  $\text{CDCl}_3$ )  $\delta$  135.2 (aromatic), 132.3 (aromatic), 130.9 (aromatic), 128.3 (aromatic), 65.3 ( $-\text{OCH}_2\text{CH}_2\text{SH}$ ), 27.3 ( $-\text{OCH}_2\text{CH}_2\text{SH}$ ).  $^{29}\text{Si}$ -NMR (99 MHz,  $\text{CDCl}_3$ )  $\delta$  -30.8 (Ph<sub>2</sub>Si-). Elemental analysis calcd for  $\text{C}_{16}\text{H}_{20}\text{O}_2\text{S}_2\text{Si}$  C 57.10, H 5.99; found C 57.41, H 6.08.

### POLYMER NETWORK SYNTHESIS

Each composition reported in this work was formed from the polymerization of thiol and alkene monomers in a molar ratio of 1:1 alkene to thiol. All polymerizations were carried out at room temperature and without solvent by photopolymerization. The initiator was 0.1 wt % DMPA of total monomer concentration dissolved in the monomer solution. During mixing, the vial was covered in aluminum foil to prevent incident light from contacting the monomer solution. Without exposing the solution to fluorescent light, the vial was mixed through vortexing and sonication until the solution was visually homogenous and without air bubbles. The monomer solution was cast between two glass slides (75 × 50 mm) separated by a glass spacer, 1.2 mm or 35  $\mu\text{m}$  thick. Polymerization was performed using a crosslinking chamber with five overhead 365 nm UV bulbs (UVP via Cole-Parmer) for 15 minutes. After polymerization each sample was postcured for 24 hours at 120 °C under a reduced pressure of -635 mTorr. After postcure, samples were stored in a desiccated chamber.

### DYNAMIC MECHANICAL ANALYSIS

DMA was performed on a Mettler Toledo DMA 861e/SDTA. Samples were cut into cylinders approximately 1.2 mm thick and ~3 mm in diameter. The mode of deformation was shear, and strain was limited to a maximum of 0.1%. Samples were

tested at a heating rate of 2 °C/min. The frequency of deformation shown is 1 Hz. Tests were conducted in a nitrogen atmosphere. It should be noted that all samples that were implanted or swollen were chosen to be appropriately sized for mechanical testing (~1 mm thick) and are not representative of the dimensions of the fabricated neural interfaces (~35 μm thick).  $T_g$  by DMA is denoted as the peak of  $\tan \delta$ . Each composition was tested at least twice. All modulus data presented here is the shear modulus. The shear modulus ( $G$ ) is related to the Young's modulus ( $E$ ) through Poisson's ratio ( $\nu$ ) as given by  $G = E/2(1 + \nu)$ . Poisson's ratio was not measured for these polymers; however  $\nu$  can be generally taken as approximately ~0.35 for glassy polymers and 0.5 for polymers above the glass transition.

#### COMPRESSION TESTING

The quasi-static compressive stress-strain response was measured using a TA instruments Discovery HR-3 rheometer with a Peltier plate heating accessory. Samples were exposed to simulated physiological conditions for between 0 hr and 48 hr. Each sample was loaded between parallel plates and preloaded to 0.03 MPa and the gap flooded with PBS. After allowing equilibration at 37 °C, the sample was deformed in compression with a strain rate of 0.06 s<sup>-1</sup> to either a maximum load of 50 N or until failure, which is indicated by an “ $\diamond$ ”. Three identical samples were tested for each composition at each time point and the data presented is representative of the three tested samples.

#### DEGRADATION MEASUREMENTS

Samples consisted of ~10 mg laser machined cylinders 3 mm in diameter and 1.2 mm tall. This sample geometry was selected for suitability of thermomechanical analysis during the degradation. The dry mass of each sample was measured and recorded with a balance with 0.01 mg precision. Equilibrium mass was measured by weight change after Each sample was individually immersed in 2 mL phosphate buffered saline at 37 °C for the recorded amount of time. At each desired time point each sample was removed from the PBS, and the surface of the polymer was gently dried using an absorbent wipe. The equilibrium mass was then recorded. Equilibrium mass change is calculated as the mass change from original mass to swollen/degraded mass normalized to the original mass. Each sample was then dried at 120 °C at a pressure of approximately 120 mTorr on a PTFE sheet to constant mass, approximately 4 hour. Each sample was then remassed. Mass loss is calculated as the mass change from the original mass to mass after drying normalized to the original mass. The water content in the network is calculated as the difference between equilibrium mass and dried mass normalized to the original mass. Data reported are the average of 3 samples at each time point. Error bars represent the standard deviation.

#### DEGRADATION PRODUCT ANALYSIS

The GC-MS chromatograms were obtained on an Agilent Technologies 6850 series II network GC system. A GC-MS vial was charged with the polymer network (0.01-0.03 g) and PBS (1.5 mL). The vial was placed in an oil bath (37-40 °C) and the degradation was monitored by GC-MS until no significant

changes were observed. The organic layer was then extracted with  $\text{CDCl}_3$  and a <sup>1</sup>H NMR was taken. The <sup>1</sup>H NMR spectra were measured on a JOEL 500 MHz NMR spectrometer and chemical shifts are reported in parts per million referenced to tetramethylsilane. The model degradation compounds were synthesized and characterized using similar methods as the polymer networks using the appropriate alkene (allyl alcohol or **3**), 2-mercaptoethanol, and DMPA.

#### SUBSTRATE PREPARATION FOR PHOTOLITHOGRAPHY

75 × 50 mm glass microscope slides were cleaned by subsequent steps of scrubbing in an Alconox solution, sonication in acetone, sonication in isopropanol and repeated as necessary until free of optically visible unwanted material. 300 nm of Au was deposited at 0.2 nm/s by physical vapor deposition (electron-beam). Subsequently 500 nm of Parylene-C was deposited on the gold. Metal and Parylene-C transfer was accomplished by using the sacrificial substrate with unpatterned film as the bottom slide for the mold with the metal surface facing inward. The top side of the mold was a cleaned glass slide coated in silicone mold release. Due to the comparatively poor adhesion of the gold to the sacrificial glass slide the metal and Parylene-C was transferred to the SMP substrate via a process previously described. After polymerization the substrate adheres sufficiently well to the top glass slide that delamination does not occur throughout processing; silicone mold release ensures that the polymer substrate will release from the carrier slide after processing.

#### METAL PATTERNING

Electrodes were then patterned by standard photolithography using S1813 photoresist (Microposit). The positive resist was spun onto the metal coated polymer at 2000 rpm with an acceleration of 3000 rpm/s. The resist was then soft-baked at 85 °C for 10 minutes. A pattern was transferred to the resist using UV light at a dose of 150 mJ/cm<sup>2</sup>. The resist was developed using MF-319 developer and subsequently hard-baked at 85 °C for 10 minutes. Metal was then etched using gold etchant (AU-5 Cyantek Corporation) diluted in a 1:1 volume ratio.

#### PARYLENE-C DEPOSITION AND PATTERNING

An additional 500 nm of Parylene-C was deposited using a Labcoater 2 (SCS Systems). Patterning of the photoresist was accomplished through similar methods described during metal patterning. Parylene-C was etched using a Technics reactive ion etching (RIE) tool using oxygen plasma. A pressure of 100 mTorr and power of 50 W was used. Each sample was etched for 9 minutes. After RIE the photoresist was removed using a flood exposure and subsequent developing.

#### DEVICE DEFINITION AND ELECTRICAL BONDING

Micromachining was performed using a 355nm diode-pumped solid-state Nd:YAG laser connected to a μFab workstation (Newport). Devices were removed from the carrier glass slide by lifting gently with a moistened razor blade. Probes were electrically bonded to a custom printed circuit board using a zero insertion force connector.

#### DYNAMIC MECHANICAL ANALYSIS

DMA was performed on a Mettler Toledo DMA 861e/SDTA. Samples were cut into cylinders approximately 1.2 mm thick

and ~3 mm in diameter. The mode of deformation was shear, and strain was limited to a maximum of 0.08%. Samples were tested at a heating rate of 2 °C/min and over the range of 0 °C – 100 °C. The frequency of deformation was 1 Hz. Tests were conducted in a nitrogen atmosphere.  $T_g$  by DMA is denoted as the peak of  $\tan \delta$ . Each composition was tested at least twice.

#### DIFFERENTIAL SCANNING CALORIMETRY

DSC on both dry and swollen samples was performed on a Mettler Toledo DSC 1 with an intracooler option. Dry samples were heated from room temperature to 125 °C, cooled to -30 °C and subsequently heated to 200 °C. Data shown are of only the second heating ramp. Swollen samples were loaded at 25 °C, cooled to -30 °C and subsequently heated to 100 °C. Data shown are of only the heating ramp. For both types of samples heating and cooling rates were fixed at 10 °C/min. Tests were conducted in a nitrogen atmosphere.  $T_g$  by DSC is denoted as the midpoint of the transition.

#### IMPEDANCE SPECTROSCOPY

Impedance spectroscopy was performed using a CH Instruments (Austin, TX) potentiostat. A 3-electrode setup was used and the tests were performed in PBS with a Ag/AgCl reference electrode and a large gold counter electrode. Frequencies between 1000 and 100,000 Hz were tested using a 5 mV sinusoidal potential.

## Conclusion

In this work we demonstrate a series of thiols and alkenes which, when appropriately combined, lead to a class of tunable, degradable biomaterials compatible with full photolithography flexible electronics processing. The resulting biopolymers demonstrate degradation profiles for which the time course is directly related to the accessibility and frequency of silyl ether linkages in the polymer network. In this way polymers are demonstrated with significant mass loss occurring selectively on the day, week, and month timescales and beyond. Furthermore, mechanical properties are compared at various time points along the degradation pathway in selected systems. Responsive, softening neural electronics are fabricated on silyl ether based degradable substrates with the intent to provide for rigid insertion, softening in the immediate time course after implantation, and subsequent long-term degradation which could lead to well-encapsulated electrodes in biologically imperceptible electronics. Future work will focus on long-term local tissue response and toxicity studies, and will ultimately move beyond in vitro analyses to validation of these materials in animal models.

## Acknowledgements

THW would like to acknowledge support from the NSF Graduate Research Fellowship. In addition, this work was supported by funding from the Texas Biomedical Device Center at The University of Texas at Dallas and the DARPA Young Faculty Award Program. The authors thank Southern Methodist University for support of this work. A.

Jennings was partially supported by a Texas Space Grant Consortium Graduate Fellowship.

THW, WV and DS would like to thank Keith Hearon, Radu Reit and Jonathan Reeder for thoughtful discussions, suggestions for future work and adjacent research with similar polymer systems that have helped to clarify and strengthen this effort.

## Notes and references

<sup>1</sup> Department of Materials Science and Engineering, The University of Texas at Dallas, 800 West Campbell RD, RL 3 Richardson, TX, 75080, USA

<sup>2</sup> Department of Chemistry, Center for Drug Discovery, Design, and Delivery (CD4), Southern Methodist University, Dallas, TX, 75275, USA

#### Author Contributions

The manuscript was written through contributions of all authors. All authors have given approval to the final version of the manuscript. ‡These authors contributed equally.

#### Present Address

† Air Force Research Laboratory, Materials and Manufacturing Directorate, Wright Patterson Air Force Base, OH, USA. & Azimuth Corporation, 4134 Linden Ave. #300, Dayton, OH 45432, USA

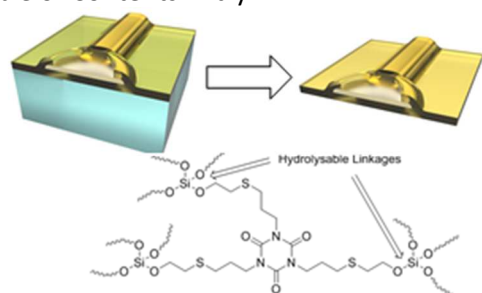
**AUTHOR DECLARATION:** Taylor Ware and Walter Voit have a significant financial interest in Syzygy Memory Plastics, Inc. This financial interest has been disclosed to UT Dallas and a conflict of interest management plan is in place to manage the potential conflict of interest associated with this research program.

Electronic Supplementary Information (ESI) is available online. See DOI: 10.1039/b000000x/

- (1) R. Langer, D.A. Tirrell, *Nature*, 2004, **428**, 487.
- (2) A. Göpferich, *Biomaterials*, 1996, **17**, 103.
- (3) S. P. Gitto, K. L. Wooley, *Macromolecules*, 1995, **28**, 8887.
- (4) J. M. Weinberg, S. P. Gitto, K. L. Wooley, *Macromolecules*, 1998, **31**, 15.
- (5) M.C. Parrott, J. C. Luft, J. D. Byrne, J. H. Fain, M. E. Napier, J. M. DeSimone, *J. Am. Chem. Soc.*, 2010, **132**, 17928.
- (6) M. Wang, Q. Zhang, K. L. Wooley, *Biomacromolecules*, 2001, **2**, 1206.
- (7) A. R. Jennings, D. Y. Son, *Chem. Commun.*, 2013, **49**, 3467.
- (8) H. C. Kolb, M. G. Finn, K. B. Sharpless, *Angew. Chemie Int. Ed.*, 2001, **40**, 2004.
- (9) C. E. Hoyle, A. B. Lowe, C. N. Bowman, *Chem. Soc. Rev.*, 2010, **39**, 1355.
- (10) M. J. Kade, D. J. Burke, C. J. Hawker, *J. Polym. Sci. Part A Polym. Chem.*, 2010, **48**, 743.
- (11) H. Wei, A. F. Senyurt, S. Jönsson, C. E. Hoyle, *J. Polym. Sci. Part A Polym. Chem.*, 2007, **45**, 822.
- (12) D. P. Nair, N. B. Cramer, T. F. Scott, C. N. Bowman, R. Shandas, *Polymer*, 2010, **51**, 4383.

- (13) A. E. Rydholm, C. N. Bowman, K. S. Anseth, *Biomaterials*, 2005, **26**, 4495.
- (14) W. D. Cook, F. Chen, Q. D. Nghiem, T. F. Scott, C. N. Bowman, S. Chaussou, L. Le Pluart, *Macromol. Symp.*, 2010; **291**, 50.
- (15) T. Ware, D. Simon, C. Liu, T. Musa, S. Vasudevan, A. M. Sloan, E. W. Keefer, R. L. Rennaker, W. Voit, *J. Biomed. Mater. Res. Part B Appl. Biomater.*, 2013, **102**, 1.
- (16) J. P. Harris, J. R. Capadona, R. H. Miller, B. C. Healy, K. Shanmuganathan, S. J. Rowan, C. Weder, D. J. Tyler, *J. Neural Eng.*, 2011, **8**, 66011.
- (17) J. Subbaroyan, D. C. Martin, D. R. Kipke, *J. Neural Eng.*, 2005, **2**, 103.
- (18) T. D. Yoshida Kozai, B. N. Langhals, P. R. Patel, X. Deng, H. Zhang, K. L. Smith, J. Lahann, N. A. Kotov, D. R. Kipke, *Nat. Mater.*, 2012, **11**, 1065.
- (19) D. H. Kim, J. Viventi, J. J. Amsden, J. Xiao, L. Vigeland, Y. S. Kim, J. A. Blanco, B. Panilaitis, E. S. Frechette, D. Contreras, D. L. Kaplan, F. G. Omenetto, Y. Huang, K. C. Hwang, M. R. Zakin, B. Litt, J. A. Rogers, *Nat. Mater.*, 2010, **9**, 511.
- (20) L. W. Tien, F. Wu, M. D. Tang-Schomer, E. Yoon, F. G. Omenetto, D. L. Kaplan, *Adv. Funct. Mater.*, 2013, **23**, 3185.
- (21) K. Brüning, H. J. Lang, *Organomet. Chem.*, 1999, **575**, 153.
- (22) C. Kim, A. Kwon, *Synthesis (Stuttg.)*, 1998, **1998**, 105.
- (23) Hwang, S.-W., Song, J.-K., Huang, X., Cheng, H., Kang, S.-K., Kim, B. H., Kim, J.-H., Yu, S., Huang, Y. and Rogers, J. A., *Adv. Mater.*, 2014, **26**, 3905.

### Table of Contents Entry



The polymerization of silyl ether containing thiols and alkenes results in tunable, degradable thermosets with potential in implantable electronics.

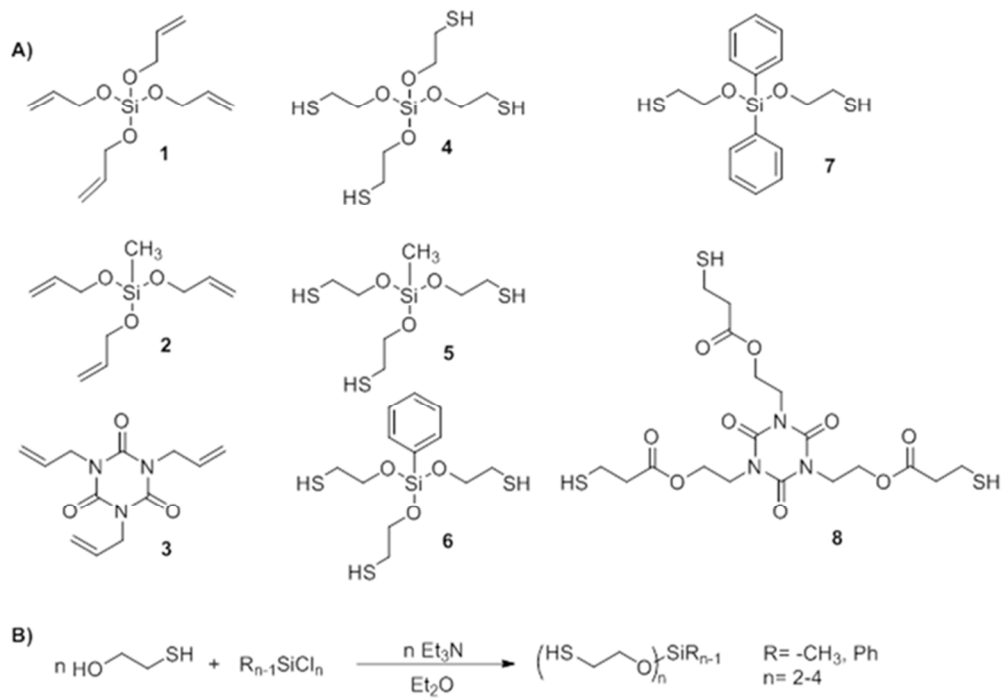


Figure 1. Pictorial representation of monomers employed in this study (A). Synthetic method used for monomers 4-7 (B).

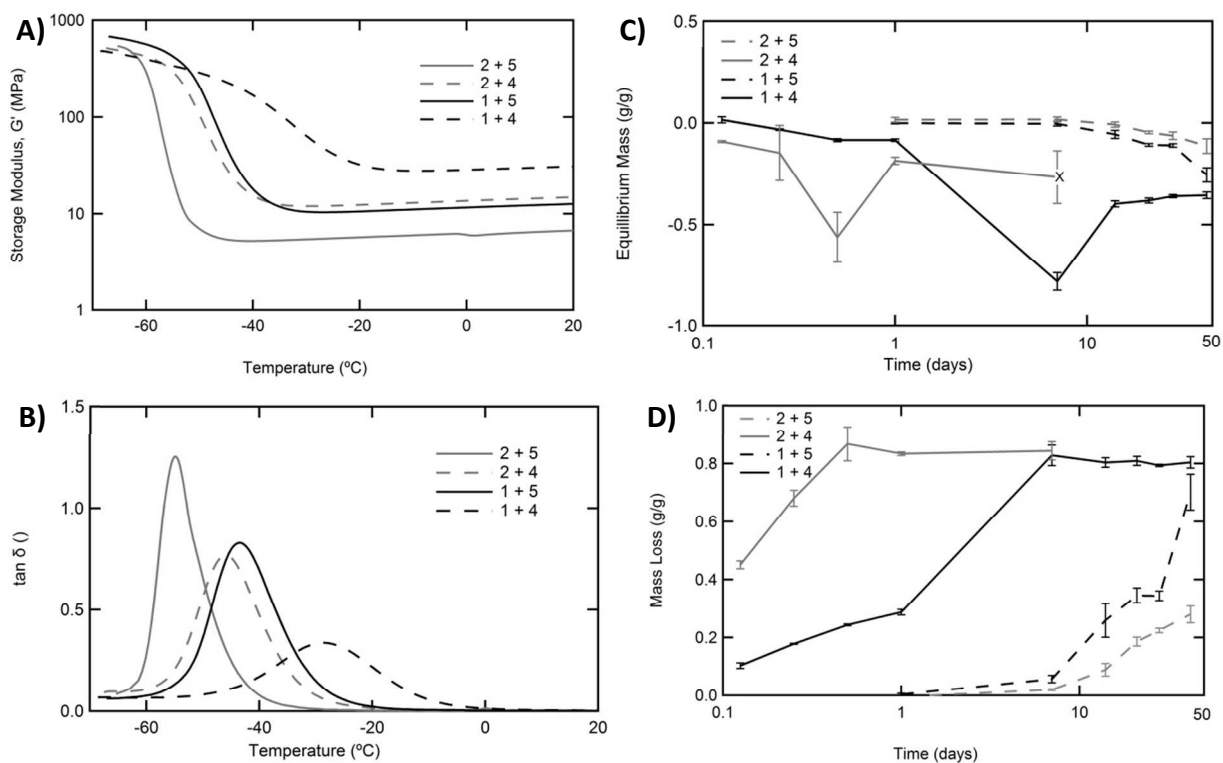


Figure 2. Dynamic mechanical analysis of polymer networks formed through radical polymerization of silyl ether containing thiols and alkenes (A,B). Degradation of these networks in simulated physiological conditions as measured by equilibrium mass (C) and total mass loss (D). In panel C and D, lines between points are only meant to guide the eye.

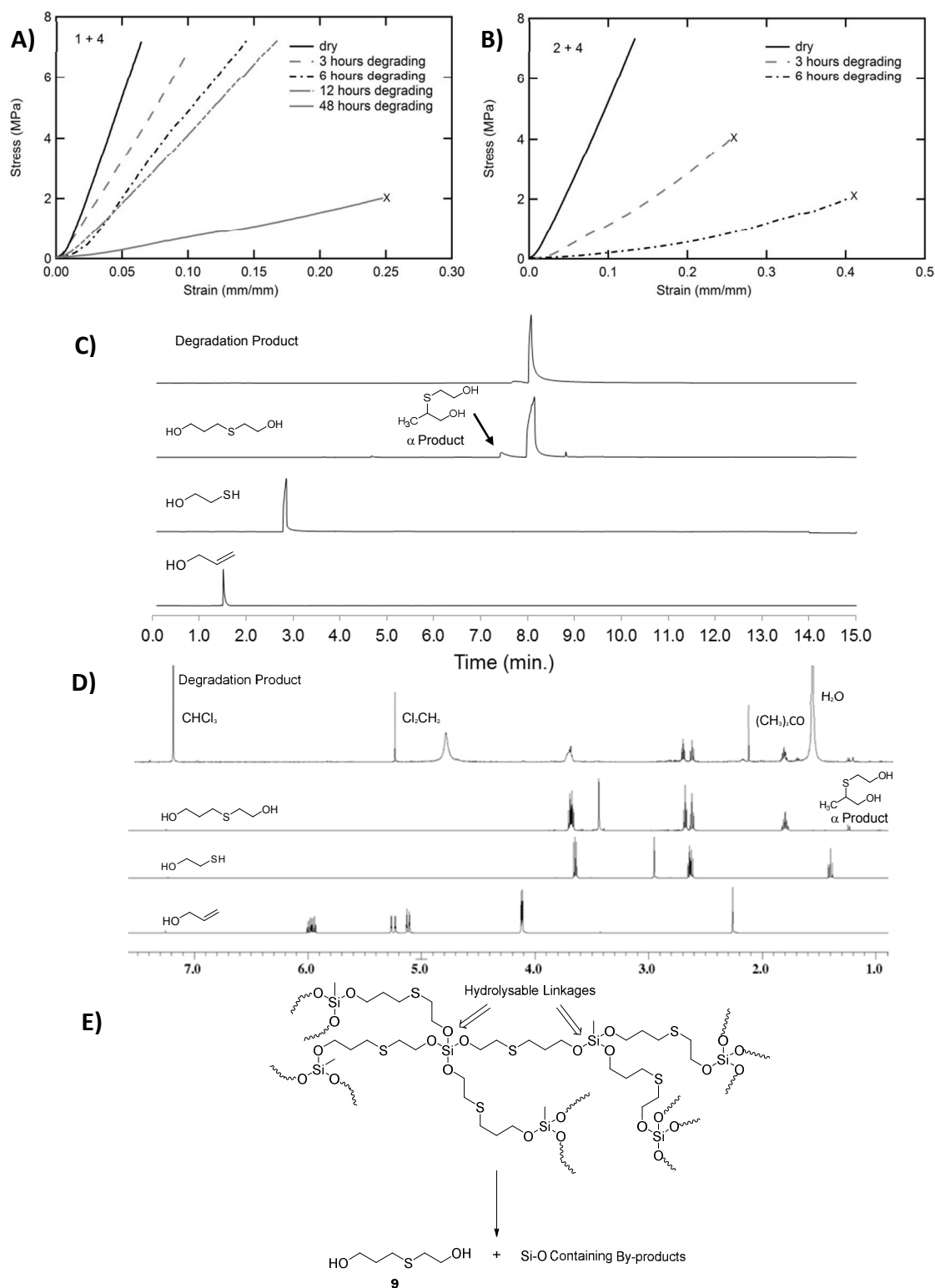


Figure 3. Compressive stress-strain analysis on two silyl ether containing polymer networks during exposure to simulated physiological conditions (A,B). Degradation products of the network formed from the polymerization of monomers 4+2 in simulated physiological conditions were characterized by GC-MS (C) and <sup>1</sup>H NMR (D) were recorded in CDCl<sub>3</sub> at 500 MHz. Schematic of the network structure and degradation products of a network formed from 4+2. (E).

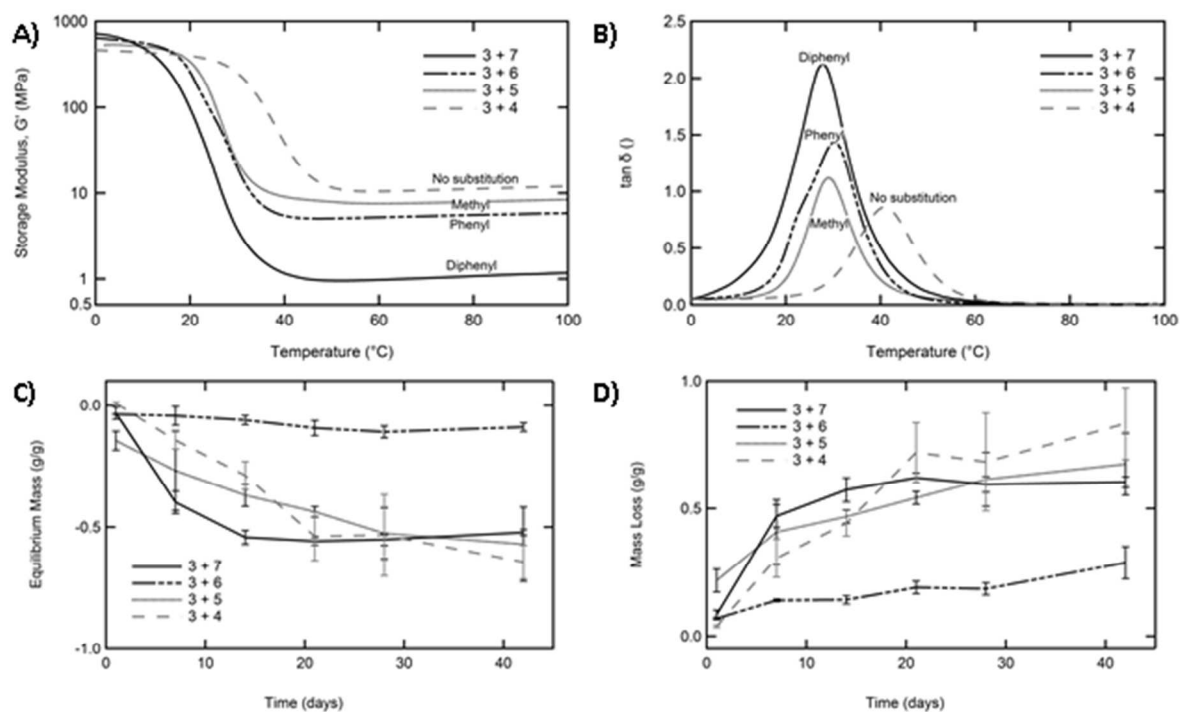


Figure 4. Dynamic mechanical analysis of networks formed with distinct silyl ether based thiols with **3** (A,B). Degradation of these networks in simulated physiological conditions as measured by equilibrium mass (C) and total mass loss (D). In panel C and D, lines between points are only meant to guide the eye.

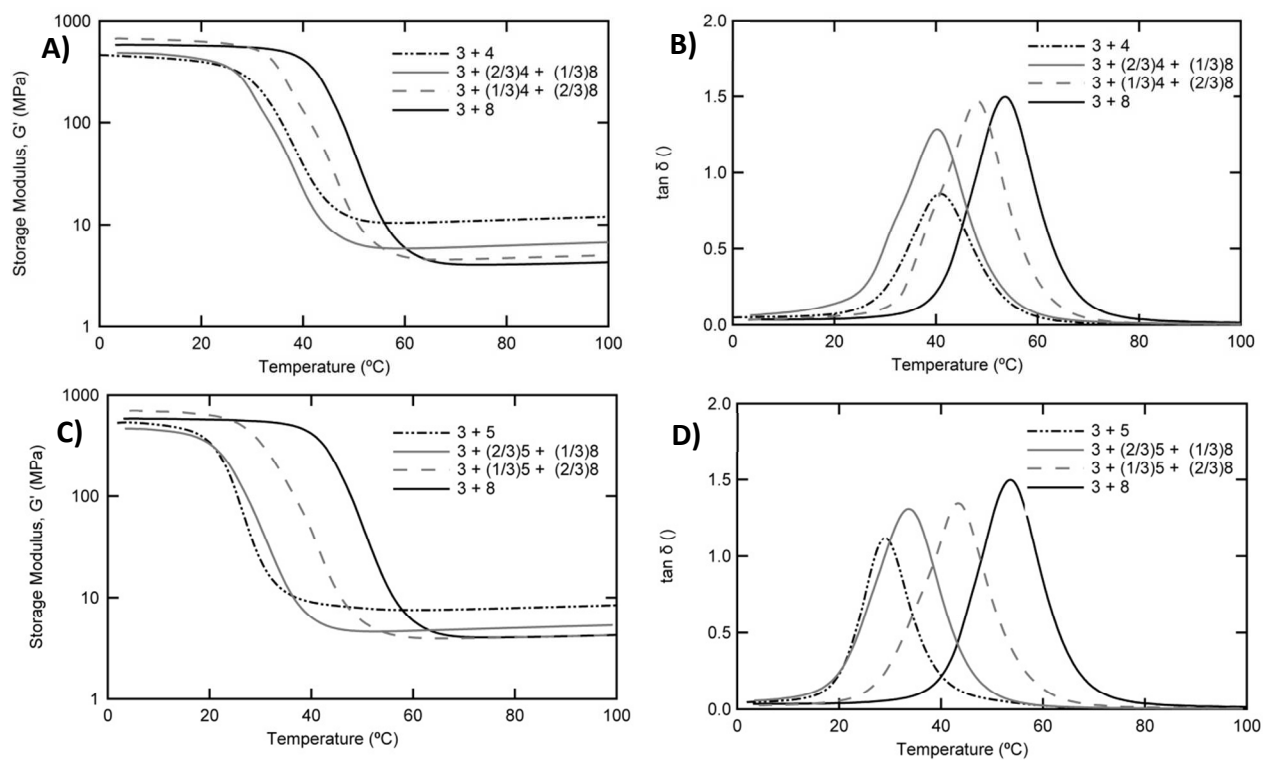


Figure 5. Dynamic mechanical analysis of networks formed with **3** and a varied amount of silyl ether thiol and a trifunctional mercaptopropionate, **8**. Tetrathiol silyl ether based polymer networks are shown in **A,C** and trithiol silyl ether based polymer networks are shown in **B,D**.

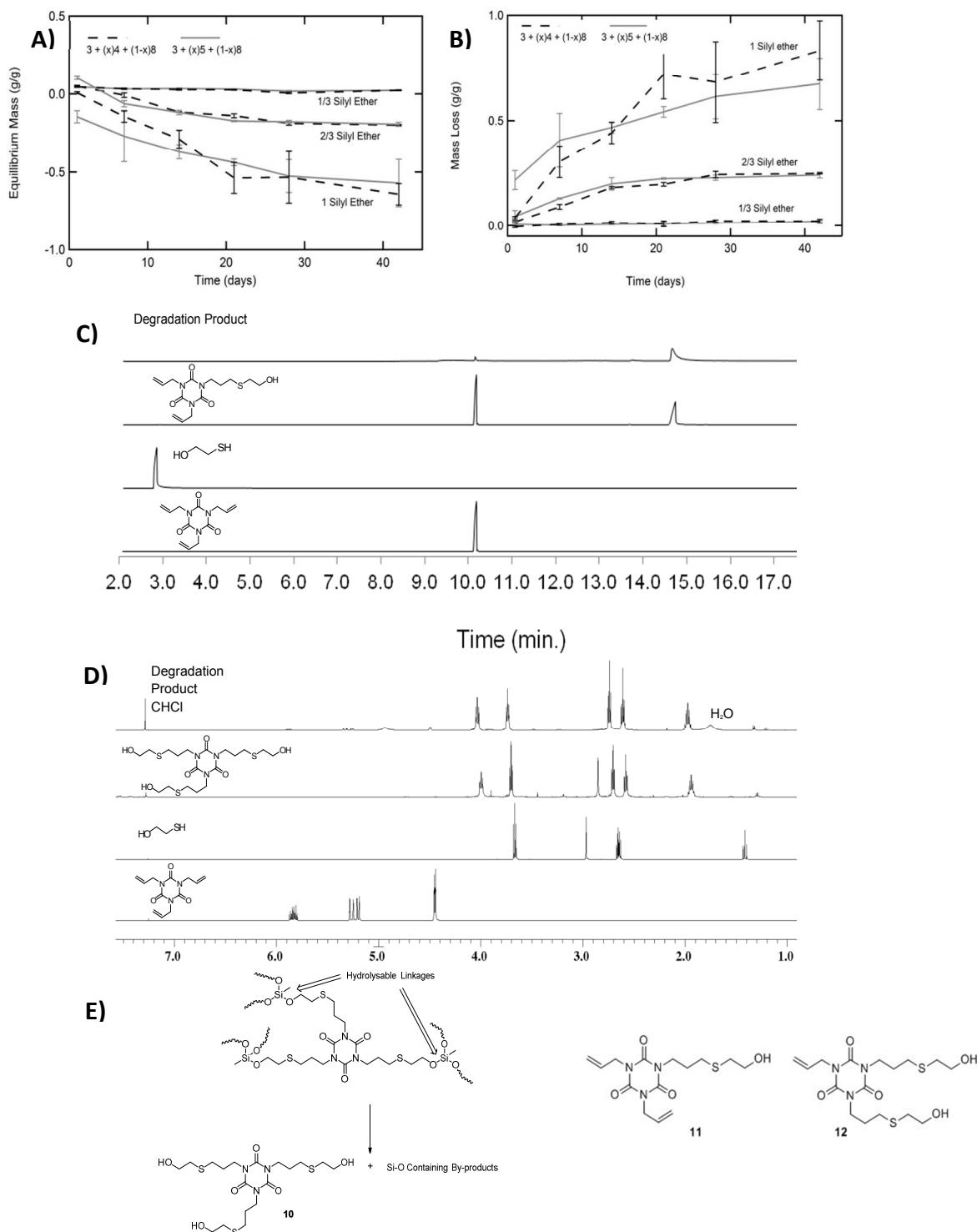


Figure 6. Degradation of networks (also shown in Figure 5) formed with **3** and a varied amount of silyl ether thiol and ester-based thiol. Degradation is characterized by equilibrium mass and mass loss for each composition (**A,B**). Degradation products of the network formed from the polymerization of monomers **5+3** in simulated physiological conditions were characterized by  $^1\text{H}$  NMR (**C**) and GC-MS (**D**). Spectra of model degradation product are shown below the measured spectra.  $^1\text{H}$  NMR were recorded in  $\text{CDCl}_3$  at 500 MHz. Schematic of the network structure and degradation products of a network formed from **5+3**. (**E**).

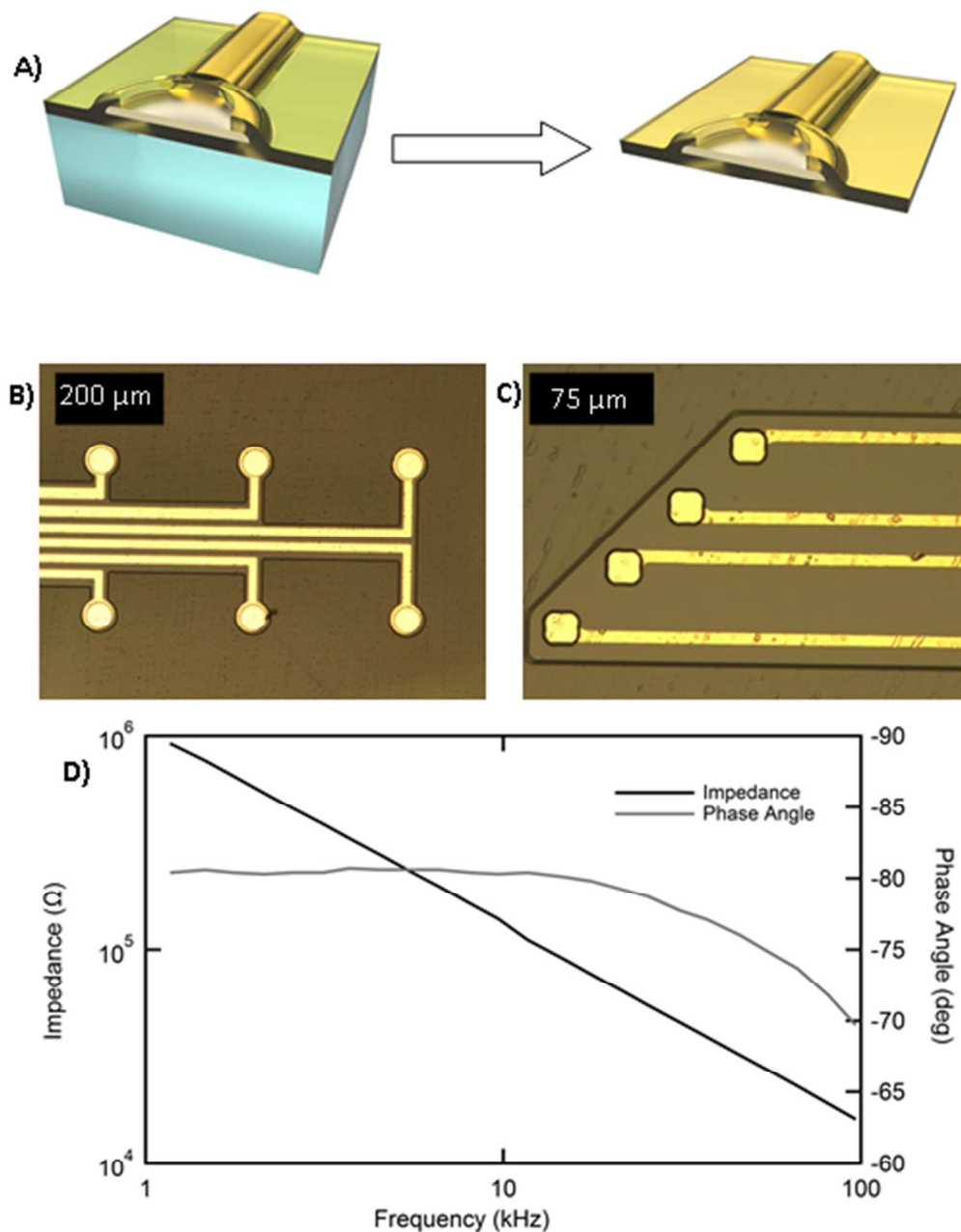


Figure 7. Schematic of the cross-section of microelectrode arrays formed by photolithography on silyl ether based degradable substrates (A). Optical micrographs of gold electrode arrays insulated with Parylene-C (B). Electrochemical impedance spectroscopy of a representative gold electrode in saline (C).